

## Numerical Analysis on Protecting Performance of Layered Arch Structures Subjected to Blast Loading

Dong Yongxiang<sup>1</sup>, Xia Changjing<sup>2,1</sup>, Feng Shunshan<sup>1</sup>, and Shao Zhiyu<sup>1</sup>

<sup>1</sup>State Key Laboratory of Explosion Science and Technology, Beijing Institute of Technology, Beijing-100 081, China

<sup>2</sup>School of Mechanics & Civil Engineering, China University of Mining & Technology, Beijing-100 083, China

### ABSTRACT

Dynamic responses of layered arch structure composed of different materials subjected to blast loading are analysed by numerical simulation. The deflection, the particle velocity and the particle acceleration of the arch inwall and stress curves versus time are obtained comparing properties of blast resistance of different arch structures with the same amount of charge. The results show that the arch structure composed of foam concrete-SFRC-steel has good blast resistance. Furthermore, the dynamic performance of the foam concrete-SFRC-steel composite structures is studied with different amount of charge. Additionally, coupling relationship of blast resistance and explosion charge is analysed. Comparison of numerical results with experimental results, show that they are in good agreement. This numerical analysis may provide important guidance for blast-resistant design and analysis of underground structures.

**Keywords:** Layered arch structure, underground structures, blast resistance, protective performance, numerical analysis

### 1. INTRODUCTION

Problems of protection of important facilities and dangerous geological environment always require urgent solutions. Particularly for underground civil and defence facilities, protection problems become difficult because of their depth from the earth's surface. Layered media, especially the sandwich material with a soft layer subjected to strong impact loading, have attracted much attention since 1970<sup>1-5</sup>. But for reason of nonlinear coupling effect of the strong impact loading with surrounding media, it is still a challenge to design reasonable protective structures. In the design of underground protective facilities, it is not enough to rely on empirical formulae as these ignore many factors and can provide very limited information. Nevertheless, numerical simulation is an effective tool to achieve reappearance of all the physical processes. 2-D and 3-D simulations of the entire process can be realised relying on the large finite element programme through the establishment of a comprehensive physical model, inputting the structural parameters and correct boundary conditions. More information can be obtained from numerical results and can provide parameters for engineering design. Therefore, protective performance of arch structure composed of different media near the explosion charge by numerical simulation has been analysed. It may provide important guidance for blast-resistant design and analysis of underground structures.

### 2. PROBLEM DESCRIPTION

For the realisation of effective protection of the underground structures close to the explosive region, different

arch structures as protective measures are adopted. The simplified model is shown in Fig. 1. Strip charge is buried in the concrete medium which is about 25 cm away from the apex of arch. On both sides of the computational model, mass blocks are located for simulating constraints of surrounding media of the realistic underground structures. Sizes of each part in Fig. 1 are shown in Table 1.

Table 1. Model sizes of arch structure

W (cm)	W <sub>2</sub> (cm)	W <sub>3</sub> (cm)	H (cm)	r (cm)
40	25	40	25.6	25

### 3. NUMERICAL SIMULATION

#### 3.1 Computational Model and Material Parameters

The problem is simplified as a 2-D plane strain problem to analyse blast resistance of middle cross-section which bears the largest loading. Using numerical simulation technique provided by LS-DYNA software, 2-D plane strain computational model was used in the numerical simulation. Compared with the 3-D model, 2-D model can save a lot of computation time and shorten the period of analysis.

In the calculation, TNT explosive, C30 concrete, C60 steel fibre-reinforced concrete (SFRC) and A3 steel plate were used. The JWL equation of state was adopted to describe the behaviour of explosion product. The Johnson-Holmquist constitutive model (JHC) was used for plain concrete and SFRC<sup>6</sup>. The crushable-foam model<sup>7</sup> was applied for foam materials. The main material parameters<sup>8-12</sup> are listed

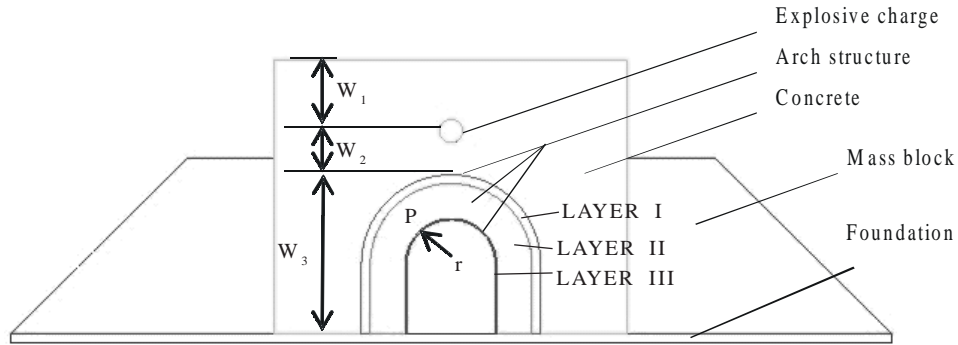


Figure 1. Sketch of analytical model.

in Tables 2 to 4. Here  $\rho$  and  $E$  are density and elastic modulus,  $D$  the detonation velocity,  $P_{CJ}$  the  $C$ - $J$  detonation pressure,  $E_0$  the internal energy per unit volume,  $\mu$  Poisson ratio and  $A, B, R_1, R_2, \omega$  are material constants of JWL equation. In Table 3,  $A', B', N$  and  $C$  are material constants determined by experiments.  $f'_c$  is the quasi-static uniaxial compressive strength.  $S_{max}$  is the normalised maximum strength which is equal to  $\sigma/f'_c$  ( $\sigma$  the actual equivalent stress).  $G$  is the shear modulus.  $D_1$  and  $D_2$  are damage constants.  $P_c = f'_c/3$  and  $\mu_l = \rho_{grain}/\rho_0 - 1$ , where  $\rho_{grain}$  is the grain density.  $\mu_c$  is the crushing volumetric strain corresponding to the pressure  $P_c$ ,  $\mu_l$  is the crushing volumetric strain corresponding to the pressure  $P_l$ .  $\epsilon_{fmin}$  is the amount of plastic strain before fracture;  $K_1, K_2$  and  $K_3$  are pressure constants,  $T$  is maximum tensile hydrostatic pressure. In Table 4,  $\sigma_c$  is the uniaxial compressive strength,  $D_{amp}$  the

damping coefficient of materials.

### 3.2 Analysis of numerical results

#### 3.2.1 Comparison of Different Arch Structures with the Same Amount of Charge

The arch structure is composed of three parts as shown in Fig. 1. Six compound modes of layered media are shown in Table 5. In different layered media, layer I, II and III are on behalf of different materials, respectively. But the total thickness of arch structure is kept constant in the investigation reported here. Except that the thickness of layer I interchanges with the thickness of layer II in group (C), the thickness of layer I, layer II, and layer III is kept constant, respectively. The thicknesses of the three layers  $H_1, H_2$  and  $H_3$  are 5 cm, 20 cm and 0.6 cm, respectively. The linear density of cylindrical TNT charge is 4.8 kg/m. The corresponding charge mass is 2 kg.

Table 2. Main parameters of the TNT explosive

$\rho$ (g/cm <sup>3</sup> )	$D$ (m/s)	$p_{CJ}$ /GPa	$A$ /GPa	$B$ /GPa	$R_1$	$R_2$	$\theta$	$E_0$ /GPa
1.63	6930	20.60	373.8	3.75	4.15	0.9	0.35	6.0

Table 3. Material constants used in calculation for plain concrete and SFRC with JHC model

Material	$\rho$ (g/cm <sup>3</sup> )	$A'$	$B'$	$N$	$C$	$f'_c$ /GPa	$S_{max}$	$G$ /GPa	$D_1$	$D_2$
Plain concrete	2.4	0.75	1.45	0.61	0.007	0.03	7.0	24.0	0.06	1.0
SFRC	2.58	0.79	1.60	0.61	0.009	0.048	7.0	24.0	0.06	1.0
Material	$\epsilon_{fmin}$	$P_c$ /GPa	$\mu_c$	$K_1$ /GPa	$K_2$ /GPa	$K_3$ /GPa	$P_l$ /GPa	$\mu_l$	$T$ /GPa	
Plain concrete	0.01	0.016	0.001	85	-171	208	0.80	0.10	0.004	
SFRC	0.05	0.016	0.001	34.4	18.8	29.8	0.80	0.10	0.013	

Table 4. Material parameters of concrete foam

Material properties	Foam aluminum	Volumetric strain	Yield stress/ MPa
$\rho$ (g/cm <sup>3</sup> )	0.72	0.0	0.0
$E$ /MPa	2.7e+02	0.02	3.2
$\mu$	0.18	0.45	7.0
$\sigma_c$ /MPa	6.0	0.55	15.0
$D_{amp}$	0.2	0.60	--

**Table 5. Compound modes of calculation model**

Group	Layer I	Layer II	Layer III
A	Plain concrete	SFRC	Steel
B	Concrete foam	SFRC	Steel
C	SFRC	Concrete foam	Steel
D	Plain concrete	SFRC	SFRC
E	A whole SFRC arch structure		
F	SFRC	SFRC	SFRC

Figures 2 to 5 show the deflection, the particle velocity and particle acceleration curves near the apex of arch *P* point (shown in Fig. 1). Figure 2 gives the displacement curve of *P* point versus time. The deflection of group (B) is the smallest which indicates that concrete foam used in layer I has a good effect on the wave attenuation. Comparing the deflection of group (B) with group (C), it can be observed that the attenuation of explosive wave of arch structure with concrete foam as layer I is better than that of arch structure with concrete foam as the middle layer. Also, it can be observed that the attenuation of group (E) is better than that of group (F) comparing the deflection of group

(E) with group (F). This result shows that though the strength of SFRC composed of one whole SFRC layer is the same as that of SFRC composed of three layers SFRC, but the stiffness of arch structures is different. The attenuation ability of group (A) with steel plate as inner layer is better than that of group (F) without the inner steel plate. From Fig. 2, it can also be seen that the deflection near *P* point of each arch structure exists an obvious fluctuation phenomenon in a long computation time because local stress wave gives rise to the vibration of the whole arch structure during a certain time under blast loading. Figure 3 shows that the extreme particle velocity of group (B) in

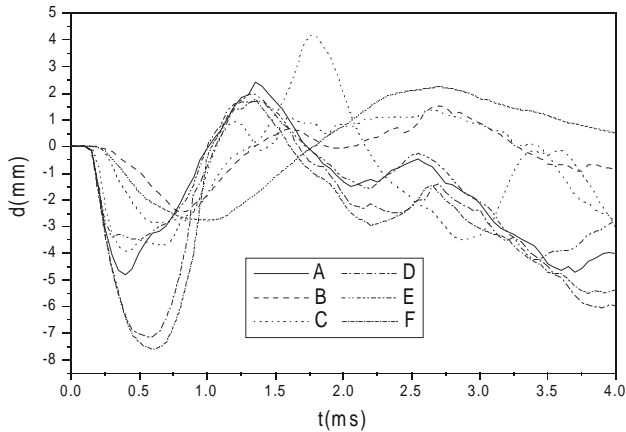


**Figure 2. Curves of deflection versus time.**

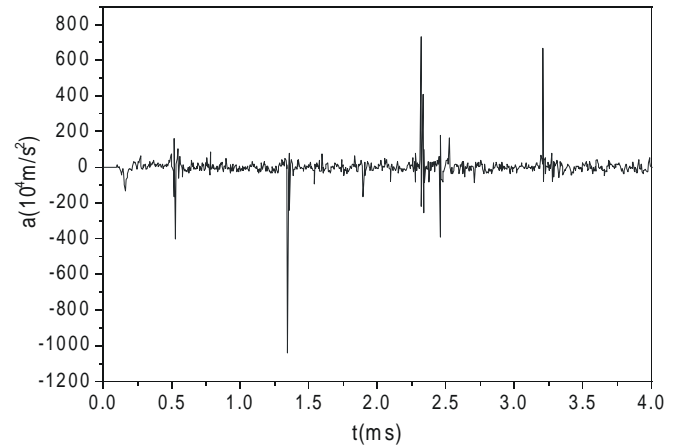


**Figure 4. Curves of acceleration of group(A).**

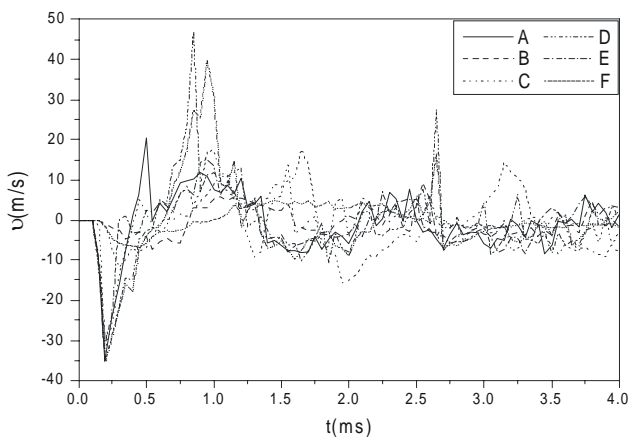


**Figure 3. Curves of particle velocity versus time.**

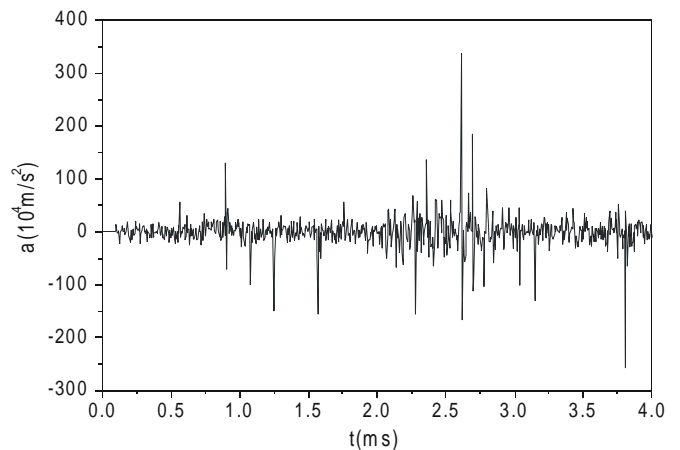


**Figure 5. Curves of acceleration of group(B).**

all curves is the smallest. Comparing the extreme velocity value curve of different arch structures, the conclusion is the same as that of the deflection in Fig. 2.

Figure 4 presents the acceleration curves versus time of group (A). The acceleration value keep zero until the explosive wave reaches the apex of arch *P* point. With the initiation of detonation, the shock wave reached arch inner wall at about 100  $\mu s$  and caused a downward acceleration. As explosive wave propagates and interacts in the arch structure, the superposition and attenuation of stress wave occur and then cause the fluctuation of wave. Figure 5 gives the acceleration curve versus time of group (B). Comparing the average acceleration of each arch structure, the average acceleration of group (B) is the smallest which shows the different attenuation values of arch structures. Numerical results further show that the average acceleration of group (A) is smaller than that of group (D). So the structure of group (A) as the inner layer with steel plate is better than the structure of group (D) without the inner steel plate.

The above analysis shows that, the protective performance of group (B) is the best. Analysis of group (B) and group (C) shows that the location of concrete foam has an important role on protective performance. When stress wave propagates through concrete foam with low-wave impedance, stress peak value decreases significantly. Under the conditions studied in this research, the earlier the explosion wave attenuates, the better the protective performance is. Therefore, whether the protective performance is better or not is determined by comprehensive consideration of structural failure criteria and the needs of practical projects.

### 3.2.2 Dynamic Responses of Arc Structure With Different Amount of Charge

The blast resistant of group (B) was analysed at three linear densities as shown in Table 5. The linear density of the cylindrical charge is 4.8 kg/m, 8.0 kg/m and 31.4 kg/m, respectively. The corresponding charge mass is 2 kg, 3.3 kg and 13.2 kg.

Figure 6 presents the deflection curve versus time of *P* point with different amount of charge. It indicates that the deflection increases as the mass of charge increases. Figure 7 gives the falling velocity versus time of *P* point. It shows that the falling velocity at large amount of charge is far faster than that at small amount of charge. Figure 8 shows that the equivalent stress of *P* point of steel plate increases with the amount of charge.

In addition, Fig. 7 shows a sharp falling of steel shell and no rebound occurs again in a short time when the amount of charge reaches a certain value for the same arch structure. The minimum amount of charge causing the rapid decrease of arch structure can be defined as the critical amount of charge. With the help of the numerical simulation, the critical amount of charge could be determined. Figure 9 gives the typical falling acceleration curve of *P* point when the linear density of the charge is 8.0 kg/m. The numerical results of group (B) at different amount of charge

show that average acceleration of *P* point increases with an increase of the linear density of charge which is in agreement with the change trends of the above deflection, velocity and stress with the amount of charge.

## 4. COMPARISON WITH EXPERIMENTS

Based on above analysis, the optimisation analysis was carried out for each layer under the same conditions as experiments. The linear density of charge is 31.4 kg/m and 8.0 kg/m, respectively. The corresponding charge mass is 13.2 kg and 3.3 kg. The composition of arch structure is shown in Fig. 10(a). The middle-layer thickness of concrete foam was 6 cm and the thicknesses of two SFRC layers were both 10 cm. The inner thickness of steel plate was 0.8 cm.

Figures 10(b) and (c) show the deformation of arch structure by simulation and experiment with 31.4 kg/m linear density of the charge. These results reveal that the images of inner layer are in good agreement.

Figure 11 gives the equivalent stress of arch structure obtained from numerical results and experiment. From Figure 11(a), it can be seen that the apex, the inwall, and the shoulder of arch structure are all the key positions to bear

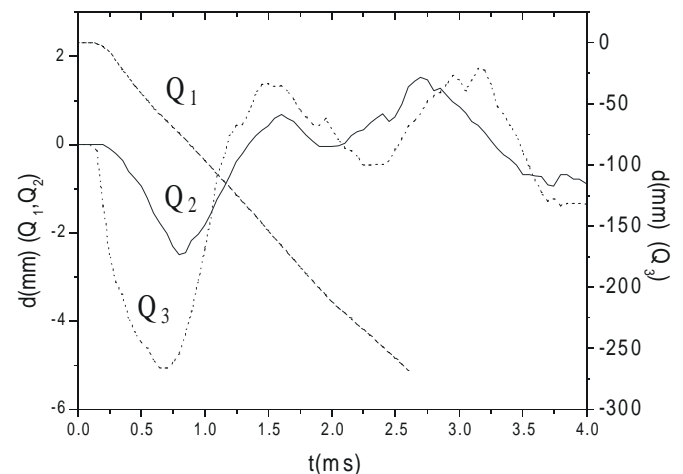


Figure 6. Deflections with different weights of charge.

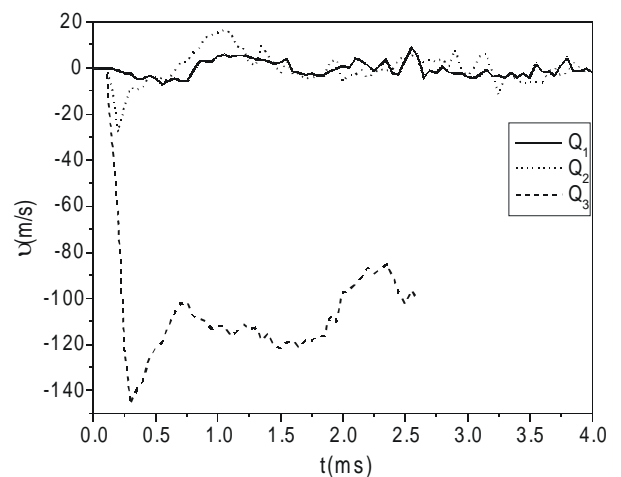


Figure 7. Velocity with different weights of charge.

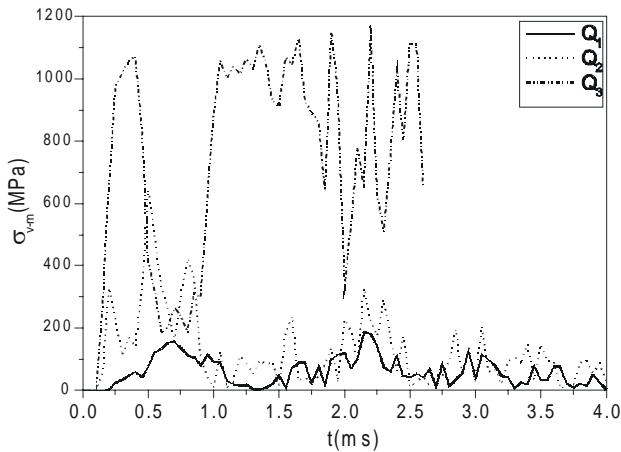


Figure 8. Curves of the equivalent stress with different amount of charge.

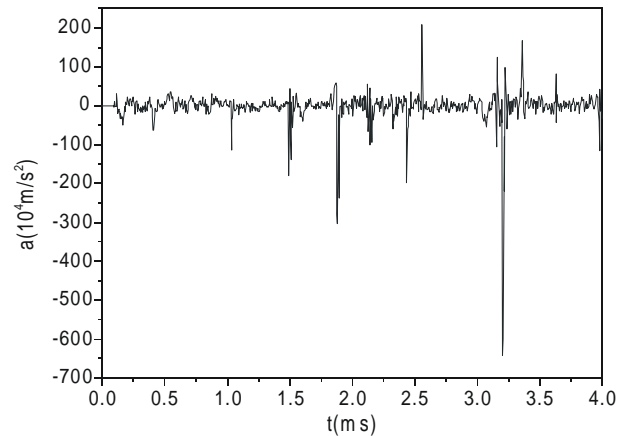


Figure 9. Typical acceleration curve with 8.0 kg/m linear density of charge.

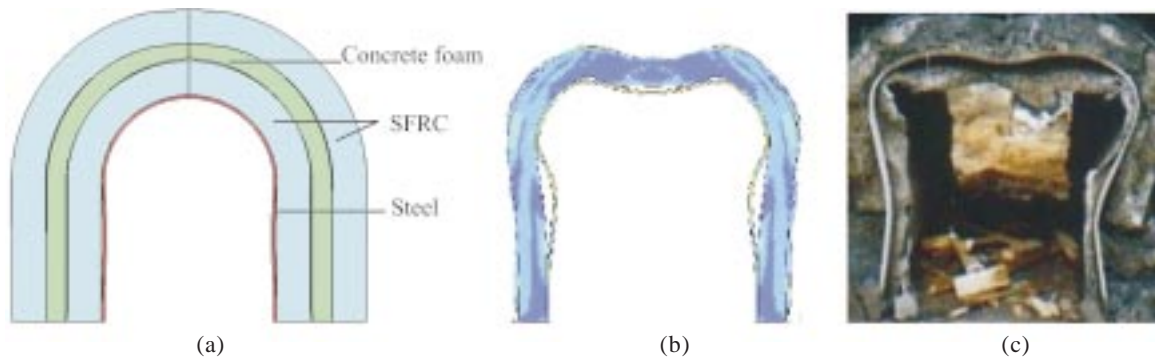


Figure 10. Comparison deformation of arc structure between simulation and experiment.

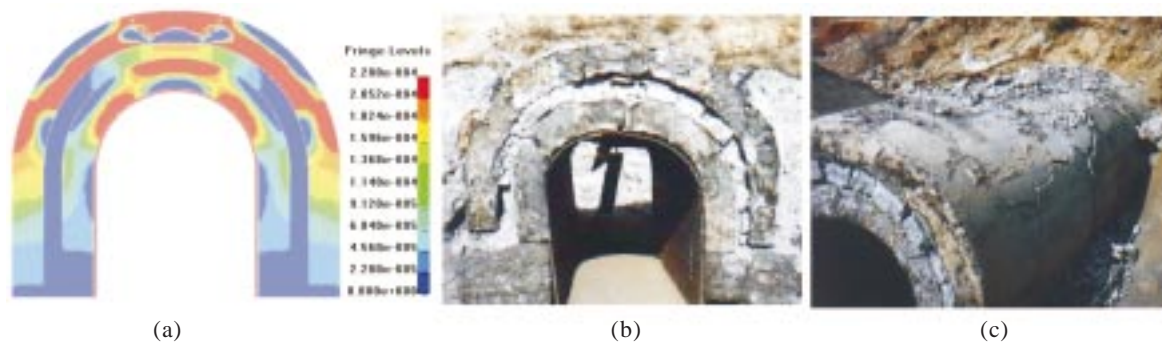


Figure 11. Typical stress state of arc structure by simulation and experiment.

the blast loading. Separation and sliding phenomena occur between two adjacent and bounding layers, and damage and cracks are easily produced in both sides of arch under the load in the arch structure [Figs 11(b) and (c)]. Numerical results are in agreement with experimental results. Therefore the corresponding measures in those weak sections could be taken for engineering design.

## 5. CONCLUSIONS

Through numerical analysis of the deformation and failure characteristics of arch structure, the physical images of the whole process of structure movement are revealed. The conclusions are as follows:

- (1) The arch structure with concrete foam has a better blast resistance as the upper layer and steel plate as an inner layer.
- (2) Comparing numerical simulation and experiments, non-dimensional deflection (the ratio of deflection of the apex to the height of arch) can be used as an index to characterise the degree of damage of the arch structure. The deflection curves of the apex, load distribution and equivalent stress curve of arch structures and the key positions to bear the blast loading are obtained from the numerical results. This provides the reference for design of arch structures.
- (3) Coupling effects between load and different layered

media have been verified by numerical simulation. Different design schemes should be adopted for different media and the structures. During design of arch structures, mis-matching principle of wave impedance and the optimum zone bearing load among media should be taken into consideration.

#### ACKNOWLEDGEMENT

The authors would like to thank Prof Z.P. Duan of Institute of Mechanics, Chinese Academy of Sciences, for the helpful discussions. This work is sponsored by Open Foundation of State Key Laboratory of Explosion Science and Technology of Beijing Institute of Technology (Grant No. KFJJ07-5).

#### REFERENCES

1. Wilkins, M. L. Mechanics of penetration and perforation. *Int. J. Eng. Sci.*, 1978, **16**(11), 793-807.
2. Tedsco, J. W.; Hayes, J. R. & Landis, D. W. Dynamic response of layered structures subject to blast effects of non-nuclear weaponry. *Comput. Struct.*, 1987, **26**, 79-86.
3. Tedsco, J.W. & Landis, D. W. Wave propagation through layered systems. *Comput. Struct.*, 1989, **26**, 625-38.
4. Franz, T.; Nurick, G. N. & Perry, M. J. Experimental investigation into the response of chopped strand mat glass fibre laminates to blast loading. *Int. J. Impact Eng.*, 2002, **27**, 639-67.
5. Serge, Abrate. Impact on laminated composites: Recent advances. *Appl. Mech. Rev.*, 1994, **47**(11), 517-44.
6. Holmquist, T. J.; Johnson, G. R. & Cook, W. H. A computational constitutive model for concrete subjected to large strains, high strain rates and high pressures. *In Fourteenth International Symposium on Ballistics*. Quebec: American Defense Preparedness Association, 1993. pp. 591-600.
7. Hallquist John, O. *In LS-DYNA Keyword user's manual*. California, Livermore Software Technology Corporation (LSTC), 2001. pp. 200-201.
8. Ma, G.W.; Hao, H. & Zhou, Y.X. Modelling of wave propagation induced by underground explosion. *Computers & Geotechnology*, 1998, **22**(3/4), 283-303.
9. Leonard E. Schwer, & Yvonne D Murray. Continuous surface cap model for geomaterial modelling: A new LS-DYNA material type. *In Seventh International LS-DYNA Users Conference*. Dearborn, Michigan, LSTC&ETA, 2002. pp. 16-35.
10. Timothy J Holmquist, *et al.* Constitutive modelling of aluminum nitride for large strain, high-strain rate, and high-pressure applications. *Int. J. Impact Eng.*, 2001, **25**, 211-31
11. Song, Shuncheng, *et al.* SPH algorithm for projectile penetrating into concrete. *Explos. Shock Waves*. 2003, **23**(1), 56-60. (in Chinese)
12. Santosa, S. P., *et al.* Experimental and numerical studies of foam-filled sections. *Int. J. Impact Eng.*, 2000, **24**, 509-34.

#### Contributors

**Dr (Ms) Dong Yongxiang** obtained her PhD from Institute of Mechanics, Chinese Academy of Sciences in 2004. In the same year, as a teacher, she joined the State Key Laboratory of Explosion Science and Technology, Beijing Institute of Technology. At present, she is working as an associate researcher and her research interests are in explosion dynamics, impact dynamics and explosion protection.

**Mr Xia Changjing** obtained his PhD from the University of Science and Technology of China in 2003. He has joined the School of Mechanics and Civil Engineering, China University of Mining and Technology in 2005. At present, he is working as an Associate Professor and his research interest is in rock mechanics and explosion dynamics.

**Mr Feng Shunshan** obtained his Masters from the Beijing Institute of Technology in 1982. He is a Professor and the leader in his chosen field of learning at State Key Laboratory of Explosion Science and Technology. His research interest include the explosive effect and its protection.

**Mr Shao Zhiyu** graduated from the Beihang University in 2007. He joined the State Key Laboratory of Explosion Science and Technology, Beijing Institute of Technology. His research interests are in smart munitions, flight dynamics, and flying control.